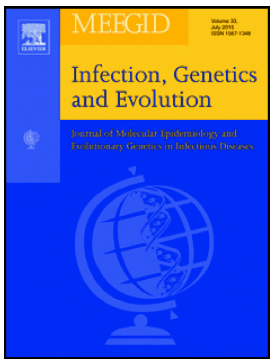

Intra-host dynamics and co-receptor usage of HIV-1 quasi-species in vertically infected patients with phenotypic switch

M.F. Fernández, M. Distefano, A. Mangano, L. Sen, P. Aulicino

PII: S1567-1348(19)30292-8

DOI: https://doi.org/10.1016/j.meegid.2019.104066

Reference: MEEGID 104066

To appear in: *Infection, Genetics and Evolution*

Received date: 20 July 2019

Revised date: 5 October 2019

Accepted date: 9 October 2019

Please cite this article as: M.F. Fernández, M. Distefano, A. Mangano, et al., Intra-host dynamics and co-receptor usage of HIV-1 quasi-species in vertically infected patients with phenotypic switch, *Infection, Genetics and Evolution*(2018), https://doi.org/10.1016/j.meegid.2019.104066

‘Intra-host dynamics and co-receptor usage of HIV-1 quasi-species in vertically infected patients with phenotypic switch’

MF. Fernández, M. Distefano, A. Mangano, L. Sen, P. Aulicino.

Laboratorio de Biología Celular y Retrovirus, Hospital de Pediatría ¨Juan P. Garrahan¨, Argentina.

Address correspondence and reprint requests to:

María Florencia Fernández
Laboratorio de Biología Celular y Retrovirus
Hospital de Pediatría “J.P. Garrahan”
Combate de los Pozos 1881
(1245) Capital Federal
República Argentina
Phone: (5411) 4308-1998
Fax number: (5411) 4122-6072
Email:mariaflor_10@hotmail.com, ffernandez@garrahan.gov.ar

Introduction

The first step of HIV-1 infection is the entry to the target cell. The attachment and subsequent infection of cells is mediated by the interaction of cellular CD4 receptor and one of two cellular co-receptors (CCR5 or CXCR4). Viruses infecting a cell via the CCR5 co-receptor are termed R5-using viruses (R5), whereas those viruses that are able to infect through CXCR4 are named X4-using viruses. Some HIV-1 strains can use both co-receptors, and are known as R5X4 or dual-tropic viruses. The ability of the virion to bind either one or both chemokine co-receptors for entry has significant implications in disease pathogenesis, and affects treatment options (Gorry, 2011). It has been shown that R5-using strains are predominantly found in HIV-1 infected patients during early or primary stages of infection, while X4-using strains are typically detected during chronic infection in approximately 50% of individuals (Koot et al., 1993), usually in association with sharp decline in CD4+ T cell counts and accelerated progession to AIDS. (Daar et al., 2007; Koot et al., 1993; Moore, 1997; Ostrowski et al., 1998; Raymond et al., 2010)

Different factors and mechanisms modulate the emergence and predominance of HIV-1 with differential co-receptor preferences during the course of infection. For example, the occupancy of CXCR4 by SDF-1/CXCL12 chemokine prevents the entry of X4-using viruses, thus blocking the activation of the fusogenic capacity of gp41 (Valenzuela-Fernández et al., 2001). Also, genetic host factors like homozygosity for the CCR5 Δ32 deletion confer resistance to R5-using viruses, restricting the infection only to viruses with tropism for the CXCR4 co-receptor (Gorry et al., 2002; Naif et al., 2002; Sheppard et al., 2002). During the course of HIV-1 infection, changes in co-receptor usage have been attributed to gradual evolutionary changes in specific regions of gp120, with emergence of intermediary dual-tropic viruses capable of infecting cells either through the CCR5 or CXCR4 co-receptors (Fouchier et al., 1992; Jensen et al., 2003). Other studies have shown that both X4- and R5-using viruses co-exist *in vivo* (van't Wout et al., 1998; Van Rij et al., 2000), and therefore changes in co-receptor usage may occur as a consequence of a differential balance of X4- and R5-using strains present within an individual.

The correlation between genetic determinants on gp120 and HIV-1 co-receptor usage has allowed the development of several scores and bioinformatic tools that predict viral tropism based on the hypervariable V3 loop sequences, either alone or in combination with clinical parameters (Westervelt et al., 1992). The importance of electrostatics for co-receptor

tropism has been previously recognized, and the best-known model, the so-called 11/25-rule, refers to charges of V3-residues 11 and 25: if one of these is positive, then the virus is associated with an X4 tropism (De Jong et al., 1992; Fouchier et al., 1992). Other differences were observed in relation to a higher net charge of the amino acids (Fouchier et al., 1992), or absence of glycosylation sites in V3 also in association with an X4 tropism (Clevestig, 2006; Pollakis et al., 2001; Polzer et al., 2002). Two classical bioinformatic tools like PSSM and Geno2pheno have been developed several years ago. These methods have very good sensitivity for predicting the tropism using V3 loop sequences of subtype B and C HIV-1 strains, and have acquired clinical relevance for prediction of HIV-1 tropism prior to initiation of antiretroviral therapy with a regimen containing the CCR5 antagonist Maraviroc.

In contrast to genotypic assays based on *in silico* predictions, phenotypic assays provide direct evidence of the presence of viruses within the viral swarm that are able to infect cells through the CCR5 and/or CXCR4 co-receptors. The most traditional phenotypic assay relies on the ability of HIV-1 to induce syncytia formation upon infection of the immortalized lymphoid cell line MT-2, that expresses CD4 and the CXCR4 co-receptor (Japour et al., 1993). Therefore, syncytium inducing viruses (SI) implies the presence of X4-using viruses while non- syncytium inducing are termed as NSI. Unlike genotypic methods, the MT-2 assay is not biased by the viral subtype. Different studies have shown discordances between phenotypic and genotypic methods (Monno et al., 2011; Saracino et al., 2010; Van Rij et al., 2000) leading to a common understanding that determinants in other regions of the envelope protein could influence HIV-1 co-receptor usage (Monno et al., 2011; Thielen et al., 2010). Indeed, mutations in V1 -V2 loop (Cashin et al., 2014; Dobrowsky et al., 2013; Pastore et al., 2006) and in gp41 (Dimonte et al., 2012) were previously associated with co-receptor usage in subtype B. Also, different potential N-linked glycosylation (PNG) sites were correlated with co-receptor usage in subtype B (Pollakis et al., 2001). However, the contribution of these determinants to viral tropism in non-B subtypes is still unclear.

Previously, we characterized the proportion of vertically infected infants with X4-using variants through phenotypic methods, showing that these strains are present in 24% of the infants less than 12 months of age, and in approximately 50% of children undergoing chronic HIV infection (Crudeli et al., 2012). A longitudinal of SI/ NSI characterization of these infants during chronic HIV infection allowed us to identify phenotypic switch in 4 cases. Thus, we sought to investigate the genotypic diversity of HIV-1 quasispecies present in these individuals, and the evolutionary changes associated with viral tropism occurring *in vivo*.

Materials and methods

Study population

The study included HIV-1 vertically infected children attending "Garrahan Pediatric Hospital," Buenos Aires, Argentina, for longitudinal follow-up of HIV-1 infection for more than ten years. A longitudinal HIV-1 phenotypic characterization was performed in 99 HIV-1 infected infants born between 1986 and 2002. Infants with phenotypic switch during the chronic stage of infection (more than 2 years after birth), and with available peripheral blood mononuclear cells (PBMC) samples, were selected for this study. We considered Informed consent from the parents or legal guardians was obtained. The study was reviewed and approved by the Ethics Committee of the Hospital (IRB 4240).

Isolation of HIV-1 from peripheral blood mononuclear cell cocultures

HIV-1 was isolated by cocultivation of cells as previously described by the AIDS Clinical Trials Group (Hollinger et al., 1992) and Crudeli, et al. (Crudeli et al., 2012). In summary, PBMCs from both the patient and HIV-1-seronegative blood donors pre-stimulated for 24–48 hours with 5 μg/ml of phytohemagglutinin (PHA) (Difco Laboratories) were co-cultured at a final concentration of 2×10^6 cells/ml. The median ratio is (1:2) between donor and patient PBMC. Co-cultures were maintained for 28 days in RPMI 1640 medium (Gibco BRL, Invitrogen) supplemented with 20% heat-inactivated fetal bovine serum (FBS), 5 U/ml interleukin-2 (IL-2) (Sigma Aldrich), and 10 μg/ml gentamicin (Gibco BRL Invitrogen), as previously described (Crudeli et al., 2012). Measurement of HIV-1 p24 Ag in co-culture supernatants was performed by microElisa assay "*HIV-1 Antigen* P24 antigen detection" (Vironostika HIV-1 Antigen, BioMérieux)

Characterization of HIV-1 phenotype on the MT-2 cell-line

The SI assay was performed as described by Crudeli, et al. (Crudeli et al., 2012). In 96-well plates, 1000 pg of p24 from HIV-1 positive cocultures were added to four wells containing 5×10^4 MT-2 cells/well in RPMI 1640 supplemented with 10% FBS and 10 μg/ml gentamicin. SI primary viral isolates and the CXCR4-tropic HIV-1 LAI Virus (from NIH AIDS Reference and Reagent Program) were used as positive controls and HIV-1BaL viral stocks were considered as negative controls. Syncytium formation of MT-2 cells was examined under light microscope every 3 days for 28 days. Since a previous study using UDS allowed us

determined that new HIV-1 variants occurred in vitro after day 28, we decided to use supernatant of day 14.

A parallel experiment was performed in order to ensure infectivity of the viral inoculum, adding the viral inoculum to wells containing 2×10^5 PHA-stimulated PBMCs from HIV-1-seronegative donors. Supernatants from all the wells were measured for HIV-1 p24 Ag. When the viral isolate infected PBMCs but was unable to induce syncytium in MT-2 cells, it was scored as NSI.

HIV *env* gene amplification, molecular cloning and Sanger sequencing

HIV *env* gene was amplified using DNA extracted from PBMCs. Briefly, a fragment of 680 base pairs comprising the C2-V5 region was amplified by nested-PCR using outer primers ED5 (5'-ATGGGATCAAAGCCTAAAGCCATGTG; positions 6556-6581) and ED12 (5'-AGTGCTTCCTGCTGCTCCCAAGAACCCAAG; positions 7822-7792) and inner primers TAG_ES7 (5'- cacgacgttgtaaaacgacCTGTTAAATGGCAGTCTAGC; positions 7001-7020) and TAG_ES8(5'-caggaaacagctatgaccCACTTCTCCAATTGTCCCTCA; positions 7647-7667) (Delwart et al., 1995). The PCR products were purified using the NucleoSpinH Extract PCR purification Kit (Macherey and Nagel) according to the manufacturer's description. The purified fragments were cloned into plasmid vectors (Topo TA Cloning, Invitrogen) and amplified in chemically competent E. coli TOP 10 (Thermo Fisher Scientific). Recombinants were selected by the blue/white method and plasmids were purified by a commercial method (Illustra Mini Spin Kit, GE Healthcare). Each clone was sequenced using the Dye Terminator v1.1 sequencing kit (Amersham Biosciences, England). Sanger sequencing reactions were analyzed with the ABI3500 automated sequencer (Applied Biosystems) and the DNA Sequencing Analysis Software v5.3.1 (Applied Biosystems, USA). The sequences were visualized and edited using FinchTV v1.4.0.

Ultra Deep Sequencing (UDS) of HIV-1 *env* C2-V5 region

UDS was performed on the 454 GS FLX System. A 800 nt amplicon was generated by PCR encompassing the C2-V5 region, the 454 sequencing adapter and Multiplex Identifier (MID) adapter. Each sample was amplified in triplicate and then pooled. The library was purified using Agencourt AMpure XP beads (Agencourt/Beckman Coulter Genomics, Danver, MA) to remove small fragments according to the Roche Amplicon Library Preparation Method Manual. Libraries were quantified using the Quant-iT PicoGreen dsDNA Assay Kit (Invitrogen)

and then pooled. Size and purity of the libraries were checked with the Agilent Bioanalyzer 2100 high sensitivity DNA chip. Each product was then diluted in TE buffer to a working stock of 10^7 molecules/µl. Pooled PCR products were clonally amplified on capture beads in water-in-oil emulsion micro-reactors, and pyrosequenced in both forward and reverse directions with Life Science platform (GS-FLX, Roche Applied Science). To estimate the UDS error rate, the *env* fragment of pNL4.3 plasmid clone was sequenced in triplicate. Then, it was aligned with the pNL4.3 sequence reference (AF324493) and the error rate was estimated with Samtools software as the number of mismatches divided by the total number of sequenced bases. The mean UDS error rate was 1.07%.

Phylogenetic analysis

For quasispecies assembly of UDS datasets, Qure program (Prosperi and Salemi, 2012) was used with an HIV-1 subtype F reference as ARMA159 (AF385936). Sanger and NGS nucleotide sequences were initially aligned using HMMER, then codon-aligned using GeneCutter, and manually adjusted. Phylogenetic trees were inferred by the maximum likelihood (ML) method with MEGA v6.0 program (Lanave et al., 1984) under the GTR+G nucleotide substitution model inferred according to the Akaike Information Criterion (AIC) statistics obtained with the jModelTest v0.1 (Posada, 2008).

Prediction of HIV-1 tropism based on V3 loop (*env*) sequences

HIV-1 co-receptor usage was inferred from the V3 nucleotide sequence contained in the C2-V5 HIV-1 *env* region by using two different algorithms: i) Geno2pheno (Lengauer et al., 2007) (FPR= 20%) based on the European consensus guidelines (Vandekerckhove et al., 2010); ii) Web PSSM (Jensen et al., 2003) with subtype B- x4r5 matrix.

Prediction of potential N-linked glycosylation (PNG) sites

Glycosylation sites in C2-V5 (*env*) were identified by the program N-Glycosite (Zhang et al., 2004), available at Los Alamos National Laboratory HIV Database website (Los Alamos National Laboratory, 2014). This tool calls potential N-linked glycosylation site when the sequence has an asparagine (N) occurring in the tripeptide sequence N-X-S or N-X-T, where X can be any amino acid except proline (P).

Sequence profiling of Non-Syncytium Inducing (NSI)/Syncytium inducing (SI) phenotype

To investigate potential associations between amino acid substitutions in the HIV-1 env C2-V5 region and phenotypic properties of HIV-1 isolates, differences in amino acid profile per

position within each patient time-point studied were assessed using the Jensen-Shannon Diversity (JSD). Significant positions were detected using a Monte Carlo permutation test (n=1000) between each time point for each patient. P-value was determined by the probability of obtaining a JSD equal to or higher than the True value after the 1000 randomization rounds. In order to make these calculations, scripts in Python were developed using Numpy and Biopython libraries.

Results

A total of 99 HIV-1 vertically infected patients from 1986 to 2002 were enrolled for characterization of viral phenotype by the MT-2 assay at our institution. Of them, 10 (10%) showed viral phenotypic switch (NSI to SI or SI to NSI). In 4 of these 10 individuals, PBMC samples were available from each of the time points when SI/ NSI phenotype had been characterized.

Table 1 shows clinical characteristics of 4 patients at the time of phenotypic characterization. All of them acquired HIV-1 infection through vertical transmission, and were undergoing chronic infection at the time of the study. Only one case was studied during infancy (3- to 4-years old), while the remaining three were studied during childhood or adolescence (between 9- and 19- years old). Time between samples ranged from 1 to 4 years. HIV-1 viral loads ranged from 3.80 to 5.90 $\log_{10}$ despite all patients were under a protease inhibitor (PI)-based antiretroviral therapy.

Moderate to severe immunosuppression was observed in 2 of the 4 cases, and 3 of them were in clinical stage C. In 3 cases, a single phenotypic change was observed (2 NSI to SI, 1 SI to NSI), while the remaining one switched from SI to NSI and back to SI during the study period.

In all cases, HIV-1 *env* fragments spanning C2 to V5 were amplified by PCR and subjected to Sanger population sequencing after molecular cloning (12 clones/sample). In 2 cases (#1 and #2), HIV-1 *env* fragments were generated with adapter-PCR primers and subjected to ultra-deep sequencing with 454 Roche technology, obtaining 5000 reads/sample in average.

In order to investigate the relative frequency of X4- and R5-using HIV-1 proviruses, HIV-1 V3 loop *env* sequences obtained by molecular cloning were submitted to PSSM (subtype B- x4r5 matrix) and Geno2pheno (FPR=20%) tropism prediction tools. However, changing the FPR cutoff to 10% or the PSSM matrix did not change results significantly.

Results are shown in Table 1. A mixture of X4- and R5- using sequences were found in at least one of the samples analyzed in 2 of the 4 studied cases. Case #3 showed the highest concordance between the phenotypic SI/NSI characterization by MT-2 assay and the genotypic V3-based predicted tropism: X4-using strains were found at 100% and 50% at T_1 and T_3 associated with SI phenotype, and 75% R5-using strains were found at T_2, associated with NSI phenotype. Similarly, case #4, showed 100% and 75% of R5-using strains at T_1 and T_2 (NSI phenotype), and 55% of X4-using strains after phenotypic switch to SI at T_3. In cases #1 and #2, V3 loop sequences predicted exclusively R5-using or X4-using strains, respectively. Of note, co-receptor usage based predictions differed between PSSM and Geno2Pheno in one case (#3), where Geno2Pheno predicted a higher number of X4-using clones at every time point studied: 0% vs 65% at T_1, 25% vs 45% at T_2, and 55% vs 100% at T_3.

In order to investigate with a high level of resolution the presence of X4- and R5-using strains within the viral quasispecies, V3 loop sequences from cases #1 and #2 were obtained by UDS and analyzed by PSSM. In case #1, we did not find any sequence identified as X4-using strains in T_1 and only a very low proportion of 1.02% (24/2300 reads) in T_2, while in case #2 X4-using strains were identified in 98.6% (T_1) and 98.4% (T_2) of the 5000 HIV-1 V3 analyzed sequences.

To better understand evolutionary relationships between the HIV-1 quasispecies with different tropism, ML phylogenetic trees of C2-V5 HIV-1 *env* sequences were constructed for each patient. Sequences obtained by UDS (cases #1 and #2) were assembled by Qure. In case #1, 54 unique sequences were retrieved. Most of the clades observed in the ML tree displayed intermingling of sequences from different sampling times, revealing the existence of different viral lineages that persist during the infection. One CCR5-using virus population at 4 years old is not closely related to another CCR5-using virus from this time (Figure 1a). Moreover, Qure recovered 86 unique sequences in case #2 (100% CXCR4-using) and we did not find any tendency of variants to cluster together neither by time points nor by PSSM predicted co-receptor usage (Figure 1b). In case #3, the tree topology was in agreement with PSSM-based co-receptor usage prediction. The phylogenetic tree showed that 12-years old CXCR4-using virus cluster was closely related to evolutionary distinct to CXCR4-using virus at 16- or 19-years old that were contained in two different clusters (Figure 1c). In case #4, the

tree topology did not show a clusters associated to HIV tropism or sampling time (Figure 1d). The phylogenetic relationship of C2-V5 *env* sequences to group M subtype reference strains showed that sequences from the 4 cases studied belonged to subtype F (data not shown).

Correlation between SI/NSI phenotype and site-specific glycoanalysis of C2-V5 region of gp120

Due to inconsistencies found between SI/NSI phenotype and viral tropism prediction based on V3 loop, we further investigated association of the gain/loss of potential N-linked glycosylation (PNG) sites in the HIV-1 C2-V5 *env* region to viral phenotype. Ten to 18 different PNGs were identified along the C2-V5 HIV-1 *env* genomic region. Most of the PNGs were found in the C2, V2 and V3 regions. Cases #3 and #4 also showed a high frequency of PNGs in the V4 and C4 region. In order to identify PNGs associated to phenotypic SI/ NSI properties of the viral strains, we looked for gains or losses of PNGs between samples with different phenotype. In case #1, PNG N332 was associated to SI phenotype, while loss of N400, N411 and N442 were associated to NSI. Patient #2 shared a similar PNG pattern, with loss of N400 and N442 also associated to NSI phenotype. In case #3, gain of a PNG in the C2 region at N289 and loss of N301 in the V3 loop were associated to SI phenotype at T1 and T3. In case #4, PNGs: N458 (C4 region) and N463 (V5 region) were associated to the SI phenotype (Figure 2).

Genotype differences in HIV-1 C2-V5 *env* region during phenotypic switch

In order to investigate genetic determinants in C2-V5 *env* region associated to SI/ NSI phenotype, we examined the amino acid composition of viral sequences from SI and NSI datasets.

Amino acid changes associated to phenotype were focused mainly in 5 positions inside C3 region (336, 340, 341, 343 and 346), 2 positions in V4 loop (402 and 412) one position in C4 (459), and one inside the V5 region (460) (Table 2). The complete list of residues showing significant differences between sequences obtained at the study time points with different phenotypic characterization can be found in Supplementary File. Remarkably, a deletion of 13 amino acids in V4 loop (398-411) was present in case #4 associated to NSI phenotype, while intact V4 loop sequences were present in SI strains.

Discussion

During chronic HIV-1 infection, the ability of HIV-1 strains to use CXCR4 co-receptors has been identified as an important determinant of disease progression (Koot et al., 1993; Muñoz-Fernández et al., 1996). However, evolutionary changes occurring during phenotypic switches have been difficult to characterize *in vivo*. In this study, we explored the genetic diversity of C2-V5 *env* sequences obtained during chronic infection from HIV-1 vertically infected individuals showing evidence of phenotypic SI/NSI switch. Vertical transmission of HIV-1 provides a unique opportunity to study evolutionary changes in the viral genome in the absence of re-infections or super-infections. In our study, we analyzed four pediatric patients with F subtype of HIV-1. Although it is a low number, each one was analyzed in more than one time-point and in depth. An exhaustive analysis of the R5 / X4 ratio and their phylogenetic relationships was carried out. Also, we studied the amino acids at different positions looking for candidates associated to viral tropism outside the V3 loop. This is the first publication showing a study in patients with phenotypic switch carrying the most prevalent HIV-1 circulating subtype in Argentina.

We observed that all individuals showed changes in HIV-1 phenotypic characteristics along the time and we expected to find an association between genotypic and phenotypic properties, as well as co-existence of HIV-1 strains with different co-receptor usage along the time of study. To our surprise, this was only observed in half of the children/ adolescents, while the other half showed no genotypic variation despite the phenotypic switch. Previously, genotypic-phenotypic discordances were identified in a group of Bunnik, et al. By using UDS, Bunnik et al, showed that X4 or R5 using variants present at a very low prevalence (<1%) could be responsible for these discordances (Bunnik et al., 2011). Other cause of these discrepancies could be the presence of dual tropic strains or R5X4 with ability to infect cells by the CCR5 or CXCR4 co-receptor which are indistinguishable by current genotypic methods and could not be evaluated in our study.

Due to the fact that genotypic methods rely on HIV-1 V3 loop sequence variations, HIV-1 subtype impacts on their ability to predict co-receptor usage (Garrido et al., 2008; Raymond et al., 2009). Previous studies have shown that this is particularly true for subtype F (Delgado et al., 2012), where a low sensitivity for detecting X4-using strains was observed. In our study, all individuals were infected with BF recombinant strains carrying subtype F *env*

segments. Therefore, prediction of HIV-1 co-receptor usage could be inaccurate, especially in cases where no X4-using strains were detected. However, detection of X4-using sequences was in fact detected in all cases, indicating the ability of bioinformatic methods to distinguish between X4- and R5-using strains. An additional confirmation of the ability of the methods to detect X4-using strains was obtained for case #1, where V3 sequences obtained from a plasma sample at T3 showed to be 100% X4-using (data not shown). The presence of X4-using viruses in plasma and R5-using in PBMCs is in agreement with an early switch of viral tropism in the progression of infection, and an early emergence of X4-using viruses that do not immediately dominate the virus population in either compartment, as has previously been suggested (Koot et al., 1996).

The MT-2 assay has been widely used to characterize the ability of HIV-1 to use the CXCR4 co-receptor. Despite its subjectivity, this method has shown a high degree of concordance (95% to 98%) with Trofile for detecting X4-using variants (Coakley et al., 2009). Although unlikely, it is possible that syncytia were not observed despite the presence of X4-using strains. However, the observation of syncytia in patients with no evidence of X4-using strains is even more difficult to explain. Therefore, the discordances found in our study encouraged us to analyze genotypic characteristics associated to viral phenotype in HIV-1 *env* regions outside the V3 loop. Our results showed statistically significant differences in 9 positions between C2 and V5 of HIV-1 *env* that were shared by 2 or more individuals. In particular, position 343, previously linked to dual/mix tropism in subtype B strains (Monno et al), was also associated to SI phenotype in 2 individuals from our study. However, amino acid changes differed between the individuals, and also from the reported ones, suggesting a role for position 343 in viral tropism. While Monno, *et al* associated dual/mix tropism with a K to A mutation, we found changes from K to R, Q or E. Subtype-specific variability may have a different impact on the molecular determinants responsible for HIV-1 co-receptor usage. Very little information is available regarding characterization of HIV-1 tropism in subtype F strains, and comparison of subtype B and F reference sequences from HIV Sequence Compendium 2018 (Los Alamos Database) revealed no amino acid conservation at none of the 8 positions identified by us. In contrast to most studies based on the analysis of genomic HIV-1 markers common to a group of individuals sharing similar characteristics, our study was based on longitudinal sequences obtained from the same individual over time. This allowed us to identify key positions that showed changes associated to the phenotypic switch. Whether these determinants are correlated with HIV-1 co-receptor usage will need

further validation. Despite our results could be biased by stochastic evolutionary events, the probability that the same position changes in different individuals is low, therefore restricting diversity to changes associated to tropism.

PNGs patterns have been associated with the strength of receptor binding and also with the phenotypic properties of the virus, suggesting a probable role in phenotypic changes over time (Pollakis et al., 2001). We found that PNGs patterns along the *env* gene differed among individuals as already shown in a study performed with 29 patients enrolled at the University Hospital of Zürich into the Swiss-Spanish Intermittent Treatment Trial (Joos et al., 2007). Some of the positions found in our study had already been reported as related to viral tropism. Such is the case for position 301, where the loss of the V3 loop N-Glycan correlates with CXCR4 co-receptor usage (Pollakis et al., 2001; Thordsen et al., 2002)**.** Whether the loss or gain of other PNGs found in this study influence viral tropism will need further evaluation.

Several studies have shown that staircase topology is typical of HIV-1 intra-host evolution (Shankarappa et al., 1999; Williamson, 2003), which suggests viral quasispecies undergo continual immune-driven selection through sequential population bottlenecks (Grenfell et al., 2004). Usually, HIV-1 intra-host genealogies of longitudinally sampled sequences display strong temporal structure, where sequences from the same sampling time tend to cluster together and are direct ancestors of sequences from the following time point (Gray et al., 2011). However, in this study the majority of clades displayed a clear intermingling of sequences from different sampling times in all cases, indicating the existence of various viral lineages that persist along the infection. Furthermore, in any case sequences from a determined sampling point constituted a monophyletic group, similar to what was found by Sede, *et al* (Sede et al., 2014). We observed independent evolution of X4 and R5 strains in 1 of the 4 patients. Most of the clades displayed intermingling of sequences from different time points and no clade defined by tropism for the patients 1, 2 and 4. These results suggested that R5- and X4-using variants continuously coexist and both virus populations may even expand. Similar findings have been reported in studies addressing the potential use of Maraviroc or neutralizing antibodies on HIV-1 strains with different tropism (Koot et al., 1996; van't Wout et al., 1998; Van Rij et al., 2000). However, during chronic infection the virus is subjected to different selection pressures that force it to mutate in order to adapt to the environment. Under the era of antiretroviral therapy, the phenotype change occurs in a small group of individuals, and is associated with poor prognosis and intrinsic resistance to

CCR5 inhibitors such as Maraviroc. Therefore, the study of genotypic and evolutionary changes that accompany biological traits conditioning HIV-1 pathogenesis and immune escape are important for the implementation of effective treatment strategies in patients with long-term HIV-1 infection and multiple treatment failures.

Acknowledgments

Supported by CONICET PIP 0475, the National Agency for the Promotion of Science and Technology (Agencia Nacional de Promoción Científica y tecnológica) (Grant PICT 2014-1373). We also thank F. Fay, S. Baquedano and J. Sfalcin (CIBIC S.A) for support with deep sequencing.

References:

Bozek, K., Thielen, A., Sierra, S., Kaiser, R., Lengauer, T., 2009. V3 loop sequence space analysis suggests different evolutionary patterns of CCR5- and CXCR4-tropic HIV. PLoS ONE 4. https://doi.org/10.1371/journal.pone.0007387

Bunnik, E.M., Swenson, L.C., Edo-Matas, D., Huang, W., Dong, W., Frantzell, A., Petropoulos, C.J., Coakley, E., Schuitemaker, H., Harrigan, P.R., van 't Wout, A.B., 2011. Detection of inferred CCR5- and CXCR4-using HIV-1 variants and evolutionary intermediates using ultra-deep pyrosequencing. PLoS Pathogens 7. https://doi.org/10.1371/journal.ppat.1002106

Cashin, K., Paukovics, G., Jakobsen, M.R., Østergaard, L., Churchill, M.J., Gorry, P.R., Flynn, J.K., 2014. Differences in coreceptor specificity contribute to alternative tropism of HIV-1 subtype C for CD4+T-cell subsets, including stem cell memory T-cells. Retrovirology 11, 4–9. https://doi.org/10.1186/s12977-014-0097-5

Clevestig, P., 2006. CCR5 use by human immunodeficiency virus type 1 is associated closely with the gp120 V3 loop N-linked glycosylation site. Journal of General Virology 87, 607–612. https://doi.org/10.1099/vir.0.81510-0

Coakley, E., Reeves, J.D., Huang, W., Mangas-Ruiz, M., Maurer, I., Harskamp, A.M., Gupta, S., Lie, Y., Petropoulos, C.J., Schuitemaker, H., Van't Wout, A.B., 2009. Comparison of human immunodeficiency virus type 1 tropism profiles in clinical samples by the trofile and MT-2 assays. Antimicrobial Agents and Chemotherapy 53, 4686–4693. https://doi.org/10.1128/AAC.00229-09

Crudeli, C.M., Aulicino, P.C., Rocco, C.A., Bologna, R., Mangano, A., Sen, L., 2012. Relevance of Early Detection of HIV Type 1 SI/CXCR4-Using Viruses in Vertically Infected Children. AIDS Research and Human Retroviruses 28, 685–692. https://doi.org/10.1089/aid.2011.0111

Daar, E.S., Kesler, K.L., Petropoulos, C.J., Huang, W., Bates, M., Lail, A.E., Coakley, E.P., Gomperts, E.D., Donfield, S.M., 2007. Baseline HIV Type 1 Coreceptor Tropism Predicts

Disease Progression. Clinical Infectious Diseases 45, 643–649. https://doi.org/10.1086/520650

De Jong, J.J., De Ronde, A., Keulen, W., Tersmette, M., Goudsmit, J., 1992. Minimal requirements for the human immunodeficiency virus type 1 V3 domain to support the syncytium-inducing phenotype: analysis by single amino acid substitution. Journal of virology 66, 6777–80. https://doi.org/1404617

Delgado, E., Fernández-García, A., Vega, Y., Cuevas, T., Pinilla, M., García, V., Sánchez, M., González, M., Sánchez, A.M., Thomson, M.M., Pérez-Álvarez, L., 2012. Evaluation of genotypic tropism prediction tests compared with in vitro co-receptor usage in HIV-1 primary isolates of diverse subtypes. Journal of Antimicrobial Chemotherapy 67, 25–31. https://doi.org/10.1093/jac/dkr438

Delwart, E.L., Herring, B., Rodrigo, A.G., 1995. heteroduplex mobility assay . Manual Supplementllll | ll Genetic Subtyping of Human Immuno- deficiency Virus Using a Heteroduplex Mobility Assay. Pcr Methods And Applications.

Dimonte, S., Babakir-Mina, M., Mercurio, F., Di Pinto, D., Ceccherini-Silberstein, F., Svicher, V., Perno, C.F., 2012. Selected amino acid changes in HIV-1 subtype-C gp41 are associated with specific gp120V3signatures in the regulation of co-receptor usage. Virus Research 168, 73–83. https://doi.org/10.1016/j.virusres.2012.06.019

Dobrowsky, T.M., Rabi, S.A., Nedellec, R., Daniels, B.R., Mullins, J.I., Mosier, D.E., Siliciano, R.F., Wirtz, D., 2013. Adhesion and fusion efficiencies of human immunodeficiency virus type 1 (HIV-1) surface proteins. Scientific Reports 3, 1–9. https://doi.org/10.1038/srep03014

Fouchier, R.A., Groenink, M., Kootstra, N.A., Tersmette, M., Huisman, H.G., Miedema, F., Schuitemaker, H., 1992. Phenotype-associated sequence variation in the third variable domain of the human immunodeficiency virus type 1 gp120 molecule. Journal of Virology 66, 3183–7.

Garrido, C., Roulet, V., Chueca, N., Poveda, E., Aguilera, A., Skrabal, K., Zahonero, N., Carlos, S., García, F., Faudon, J.L., Soriano, V., De Mendoza, C., 2008. Evaluation of eight different bioinformatics tools to predict viral tropism in different human immunodeficiency virus type 1 subtypes. Journal of Clinical Microbiology 46, 887–891. https://doi.org/10.1128/JCM.01611-07

Gorry, P.R., Zhang, C., Wu, S., Kunstman, K., Trachtenberg, E., Phair, J., Wolinsky, S., Gabuzda, D., 2002. Persistence of dual-tropic HIV-1 in an individual homozygous for the CCR5Δ32 allele. Lancet 359, 1832–1834. https://doi.org/10.1016/S0140-6736(02)08681-6

Gray, R.R., Pybus, O.G., Salemi, M., 2011. Measuring the temporal structure in serially sampled phylogenies. Methods in Ecology and Evolution 2, 437–445. https://doi.org/10.1111/j.2041-210X.2011.00102.x

Grenfell, B.T., Pybus, O.G., Gog, J.R., Wood, J.L.N., Daly, J.M., Mumford, J.A., Holmes, E.C., 2004. Unifying the Epidemiological and Evolutionary Dynamics of Pathogens. Science 303, 327–332. https://doi.org/10.1126/science.1090727

Hollinger, F., Bremer, J., Myers, L., Gold, J., McQuay, L., 1992. Standardization of sensitive

human immunodeficiency virus coculture procedures and establishment of a multi-center quality assurance program for the AIDS Clinical Trials Group. J 30, 1787–1794.

Japour, a J., Mayers, D.L., Johnson, V. a, Kuritzkes, D.R., Beckett, L. a, Arduino, J.M., Lane, J., Black, R.J., Reichelderfer, P.S., D'Aquila, R.T., 1993. Standardized peripheral blood mononuclear cell culture assay for determination of drug susceptibilities of clinical human immunodeficiency virus type 1 isolates. The RV-43 Study Group, the AIDS Clinical Trials Group Virology Committee Resistance Working G. Antimicrobial agents and chemotherapy 37, 1095–1101. https://doi.org/10.1128/AAC.37.5.1095

Japour, A.J., Fiscus, S.A., Arduino, J.M., Mayers, D.L., Reichelderfer, P.S., Kuritzkes, D.R., 1994. Standardized microtiter assay for determination of syncytium-inducing phenotypes of clinical human immunodeficiency virus type 1 isolates. Journal of Clinical Microbiology 32, 2291–2294.

Jensen, M.A., Li, F.-S., van 't Wout, A.B., Nickle, D.C., Shriner, D., He, H.-X., McLaughlin, S., Shankarappa, R., Margolick, J.B., Mullins, J.I., 2003. Improved Coreceptor Usage Prediction and Genotypic Monitoring of R5-to-X4 Transition by Motif Analysis of Human Immunodeficiency Virus Type 1 env V3 Loop Sequences. Journal of Virology 77, 13376–13388. https://doi.org/10.1128/JVI.77.24.13376-13388.2003

Joos, B., Fischer, M., Schweizer, A., Kuster, H., Böni, J., Wong, J.K., Weber, R., Trkola, A., Günthard, H.F., 2007. Positive In Vivo Selection of the HIV-1 Envelope Protein gp120 Occurs at Surface-Exposed Regions. The Journal of Infectious Diseases 196, 313–320. https://doi.org/10.1086/518935

Koot, M., Angélique, Van 't Wout, B., Kootstra, N.A., De Goede, R.E.Y., Tersmette, M., Schuitemaker, H., 1996. Relation between changes in cellular load, evolution of viral phenotype, and the clonal composition of virus populations in the course of human immunodeficiency virus type 1 infection. Journal of Infectious Diseases 173, 349–354. https://doi.org/10.1093/infdis/173.2.349

Koot, M., Keet, I.P.M., Vos, A.H. V, de Goede, R.E.Y., Roos, M.T.H., Coutinho, R.A., Miedema, F., Schellekens, P.T.A., Tersmette, M., 1993. Prognostic value of human immunodeficiency virus type 1 biological phenotype for rate of CD4+ cell depletion and progression to AIDS. Annals of Internal Medicine 118, 681–688.

Lanave, C., Preparata, G., Saccone, C., Serio, G., 1984. A new method for calculating evolutionary substitution rates. Journal of molecular evolution 20, 86–93. https://doi.org/10.1007/BF02101990

Lengauer, T., Sander, O., Sierra, S., Thielen, A., Kaiser, R., 2007. Bioinformatics prediction of HIV coreceptor usage. Nature Biotechnology 25, 1407–1410. https://doi.org/10.1038/nbt1371

Los Alamos National Laboratory, 2014. N-GlycoSite [WWW Document]. URL https://www.hiv.lanl.gov/content/sequence/GLYCOSITE/glycosite.html (accessed 6.20.18).

Monno, L., Annalisa, S., Scudeller, L., Punzi, G., Brindicci, G., Altamura, M., Lagioia, A., Ladisa, N., Angarano, G., 2011. Impact of mutations outside the V3 region on coreceptor tropism phenotypically assessed in patients infected with HIV-1 subtype B. Antimicrobial Agents and Chemotherapy 55, 5078–5084.

https://doi.org/10.1128/AAC.00743-11

Moore, J.P., 1997. Coreceptors: Implications for HIV Pathogenesis and Therapy. Science (New York, N.Y.) 276, 51–52.

Muñoz-Fernández, M.Á., Obregón, E., Navarro, J.M., Börner, C., Gurbindo, M.D., Sampelayo, T.H., Fernandez-cruz, E., 1996. Relationship of Virologic, Immunologic, and Clinical Parameters in Infants with Vertically Acquired Human Immunodeficiency Virus Type 1 Infection. Pediatric Research 40, 597–602.

Naif, H.M., Cunningham, A.L., Alali, M., Li, S., Nasr, N., Buhler, M.M., Schols, D., Clercq, D., Stewart, G., Clercq, E. De, 2002. A Human Immunodeficiency Virus Type 1 Isolate from an Infected Person Homozygous for CCR5 Δ 32 Exhibits Dual Tropism by Infecting Macrophages and MT2 A Human Immunodeficiency Virus Type 1 Isolate from an Infected Person Homozygous for CCR5 ⌬ 32 Exhibits D. Journal of virology 76, 3114–3124. https://doi.org/10.1128/JVI.76.7.3114

Ostrowski, M. a, Justement, S.J., Catanzaro, a, Hallahan, C. a, Ehler, L. a, Mizell, S.B., Kumar, P.N., Mican, J. a, Chun, T.W., Fauci, a S., 1998. Expression of chemokine receptors CXCR4 and CCR5 in HIV-1-infected and uninfected individuals. Journal of immunology (Baltimore, Md. : 1950) 161, 3195–201.

Pastore, C., Nedellec, R., Ramos, A., Pontow, S., Ratner, L., Mosier, D.E., 2006. Human Immunodeficiency Virus Type 1 Gain-of-Fitness Mutations Compensate for V3 Loss-of-Fitness Mutations Human Immunodeficiency Virus Type 1 Coreceptor Switching : V1 / V2 Gain-of-Fitness Mutations Compensate for V3 Loss-of-Fitness Mutations †. Society 80, 750–758. https://doi.org/10.1128/JVI.80.2.750

Paul R. Gorry, P.A., 2011. Coreceptors and HIV-1 Pathogenesis. Curr HIV/AIDS Rep 8, 45–53. https://doi.org/10.1007/s11904-010-0069-x

Pollakis, G., Kang, S., Kliphuis, A., Chalaby, M.I.M., Goudsmit, J., Paxton, W.A., 2001. N-Linked Glycosylation of the HIV Type-1 gp120 Envelope Glycoprotein as a Major Determinant of CCR5 and CXCR4 Coreceptor Utilization. Journal of Biological Chemistry 276, 13433–13441. https://doi.org/10.1074/jbc.M009779200

Polzer, S., Dittmar, M.T., Schmitz, H., Schreiber, M., 2002. The N-linked Glycan g15 within the V3 Loop of the HIV-1 External Glycoprotein gp120 Affects Coreceptor Usage , Cellular Tropism , and Neutralization 80, 70–80. https://doi.org/10.1006/viro.2002.1760

Posada, D., 2008. jModelTest: Phylogenetic model averaging. Molecular Biology and Evolution 25, 1253–1256. https://doi.org/10.1093/molbev/msn083

Prosperi, M.C.F., Salemi, M., 2012. QuRe: Software for viral quasispecies reconstruction from next-generation sequencing data. Bioinformatics 28, 132–133. https://doi.org/10.1093/bioinformatics/btr627

Raymond, S., Delobel, P., Mavigner, M., Cazabat, M., Encinas, S., Souyris, C., Bruel, P., Sandres-Sauné, K., Marchou, B., Massip, P., Izopet, J., 2010. CXCR4-using viruses in plasma and peripheral blood mononuclear cells during primary HIV-1 infection and impact on disease progression. Aids 24, 2305–2312. https://doi.org/10.1097/QAD.0b013e32833e50bb

Raymond, S., Delobel, P., Mavigner, M., Cazabat, M., Souyris, C., Encinas, S., Sandres-Sauné, K., Pasquier, C., Marchou, B., Massip, P., Izopet, J., 2009. Genotypic prediction of human immunodeficiency virus type 1 CRF02-AG tropism. Journal of Clinical Microbiology 47, 2292–2294. https://doi.org/10.1128/JCM.02439-08

Saracino, A., Monno, L., Brindicci, G., Trillo, G., Altamura, M., Punzi, G., Lagioia, A., Angarano, G., 2010. Are the proposed env mutations actually associated with resistance to maraviroc. Journal of Acquired Immune Deficiency Syndromes 53, 550–552. https://doi.org/10.1097/QAI.0b013e3181ba1c48

Sede, M.M., Moretti, F.A., Laufer, N.L., Jones, L.R., Quarleri, J.F., 2014. HIV-1 tropism dynamics and phylogenetic analysis from longitudinal ultra-deep sequencing data of CCR5- and CXCR4-using variants. PLoS ONE 9, 1–14. https://doi.org/10.1371/journal.pone.0102857

Shankarappa, R., Margolick, J.B., Gange, S.J., Rodrigo, A.G., Upchurch, D., Farzadegan, H., Gupta, P., Rinaldo, C.R., Learn, G.H., He, X., Huang, X.L., Mullins, J.I., 1999. Consistent viral evolutionary changes associated with the progression of human immunodeficiency virus type 1 infection. Journal of virology 73, 10489–502.

Sheppard, H.W., Celum, C., Michael, N., O Brien, S., Dean, M., Csrrington, M., Dondero, D., Buchbinder, S.P., 2002. HIV-1 Infection in individuals with the CCR5-delta32/delta32 genotype: Acquisition of Syncytium-Inducting virus at seroconversion. Jounal Of Acquired Immune Deficiency Syndromes 29, 307–313.

Thielen, A., Sichtig, N., Kaiser, R., Lam, J., Harrigan, P.R., Lengauer, T., 2010. Improved Prediction of HIV-1 Coreceptor Usage with Sequence Information from the Second Hypervariable Loop of gp120. The Journal of Infectious Diseases 202, 1435–1443. https://doi.org/10.1086/656600

Thordsen, I., Polzer, S., Schreiber, M., 2002. Infection of cells expressing CXCR4 mutants lacking N-glycosylation at the N-terminal extracellular domain is enhanced for R5X4-dualtropic human immunodeficiency virus type-l. BMC Infectious Diseases 2, 1–11. https://doi.org/10.1186/1471-2334-2-31

Valenzuela-Fernández, A., Palanche, T., Amara, A., Magerus, A., Altmeyer, R., Delaunay, T., Virelizier, J.L., Baleux, F., Galzi, J.L., Arenzana-Seisdedos, F., 2001. Optimal Inhibition of X4 HIV Isolates by the CXC Chemokine Stromal Cell-derived Factor 1α Requires Interaction with Cell Surface Heparan Sulfate Proteoglycans. Journal of Biological Chemistry 276, 26550–26558. https://doi.org/10.1074/jbc.M100411200

van't Wout, A B. Coakley, E., Reeves, J., Huang, W., Petropoulos, C.J., Schuitemaker, H., 2008. Dynamics of emergence of CXCR4-using HIV in clinical samples as detected by Trofile and MT-2 assays. Antiviral Therapy 13, A93.

van't Wout, A.B., Ran, L.J., Kuiken, C.L., Kootstra, N.A., Pals, S.T., Schuitemaker, H., 1998. Analysis of the temporal relationship between human immunodeficiency virus type 1 quasispecies in sequential blood samples and various organs obtained at autopsy. Journal of virology 72, 488–96.

Van Rij, R.P., Blaak, H., Visser, J.A., Brouwer, M., Rientsma, R., Broersen, S., De Roda Husman, A.M., Schuitemaker, H., 2000. Differential coreceptor expression allows for independent evolution of non-syncytium-inducing and syncytium-inducing HIV-1.

Journal of Clinical Investigation 106, 1039–1052. https://doi.org/10.1172/JCI7953

Vandekerckhove, L., Wensing, A., Kaiser, R., Brun-Vezinet, F., Clotet, B., De Luca, a, Dressler, S., Garcia, F., Geretti, A., Klimkait, T., Korn, K., Masquelier, B., Perno, C., Schapiro, J., Soriano, V., Sönnerborg, a, Vandamme, À., Verhofstede, C., Walter, H., Zazzi, M., Boucher, C., 2010. Consensus statement of the European guidelines on clinical management of HIV-1 tropism testing. Journal of the International AIDS Society 13, O7. https://doi.org/10.1186/1758-2652-13-S4-O7

Westervelt, P., Trowbridge, D.B., Epstein, L.G., Blumberg, B.M., Li, Y., Hahn, B.H., Shaw, G.M., Price, R.W., Ratner, L., 1992. Macrophage tropism determinants of human immunodeficiency virus type 1 in vivo. J Virol 66, 2577–2582.

Williamson, S., 2003. Adaptation in the env gene of HIV-1 and evolutionary theories of disease progression. Molecular Biology and Evolution 20, 1318–1325. https://doi.org/10.1093/molbev/msg144

Zhang, M., Gaschen, B., Blay, W., Foley, B., Haigwood, N., Kuiken, C., Korber, B., 2004. Tracking global patterns of N-linked glycosylation site variation in highly variable viral glycoproteins: HIV, SIV, and HCV envelopes and influenza hemagglutinin. Glycobiology 14, 1229–1246. https://doi.org/10.1093/glycob/cwh106

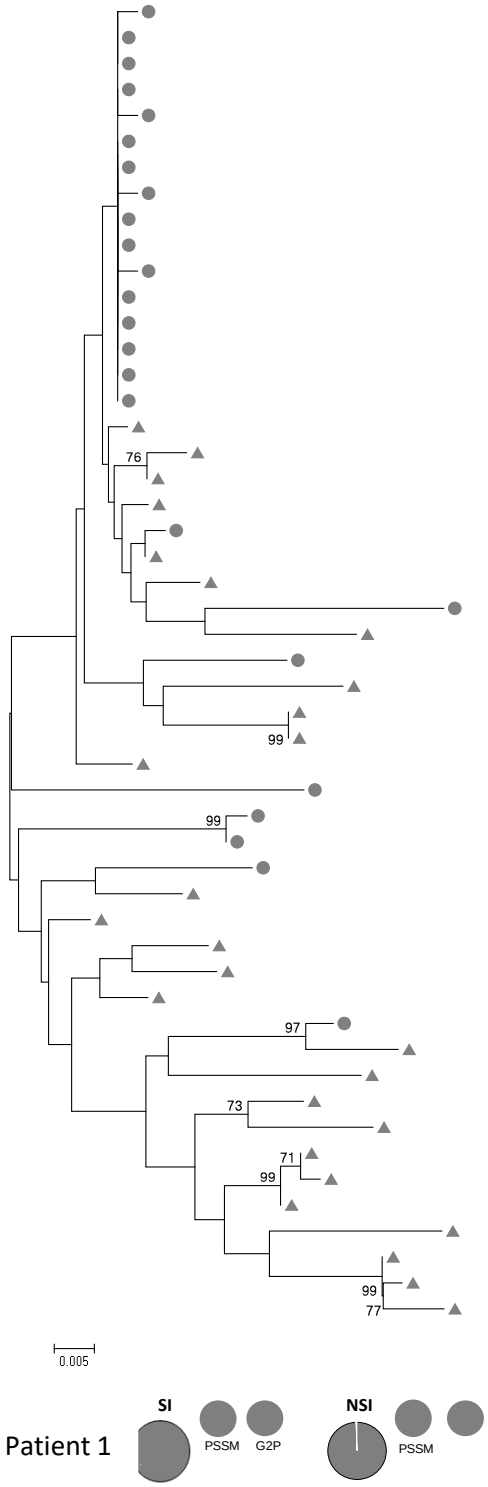

Figure 1a Maximum likelihood phylogenetic trees of proviral nucleotide sequences of C2-V5 *env* gene showing sampling time and tropism. The circles and triangles represent the quasispecies present at 3- and 4-years old, respectively. Filled symbols correspond to R5-using strains. The figure under the phylogentic tree represents the proportion of X4 and R5 HIV-1 strains of patient 1 at different times of infection. Big circles represent sequences obtained by NGS results and small circles the molecular cloning results. Gray filled circles denote R5-using strains and white filled circles X4-using strains.

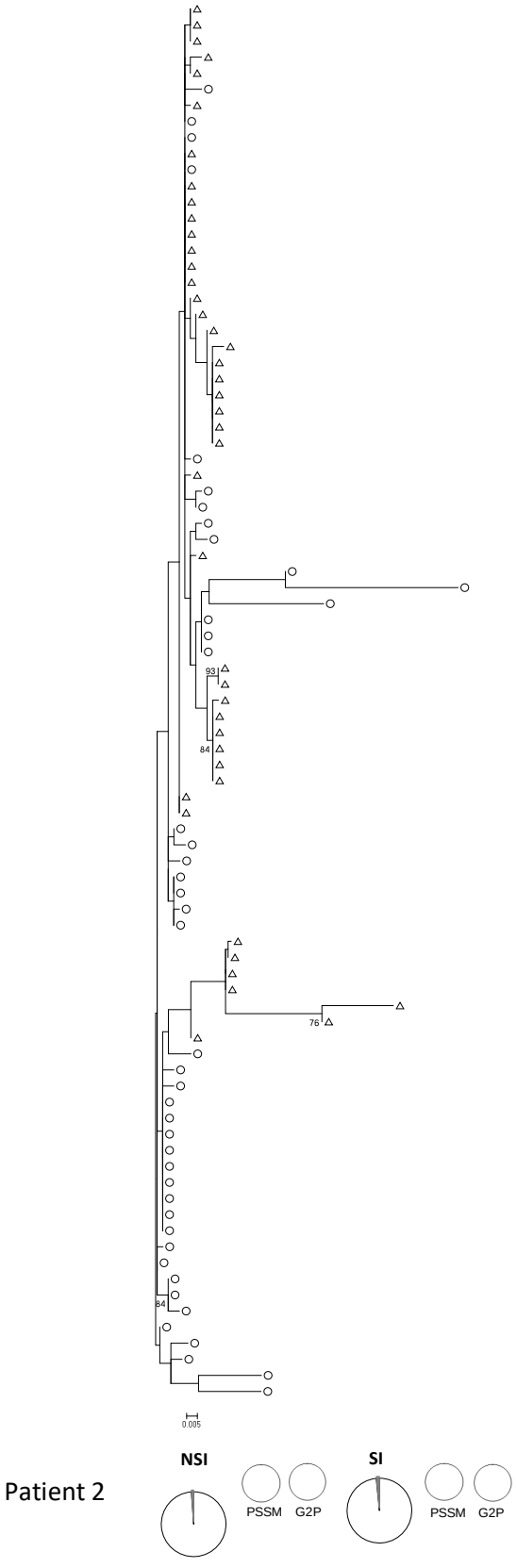

Patient 2

Figure 1b Maximum likelihood phylogenetic trees of proviral nucleotide sequences of C2-V5 HIV *env* gene showing sampling time and tropism. The circles and triangles represent the quasispecies present at 10- and 11-years old, respectively. Empty symbols correspond to X4-using strains. The figure under the phylogentic tree represents the proportion of X4 and R5 HIV-1 strains of patient 2 at different times of infection. Big circles represent sequences obtained by NGS results and small circles the molecular cloning results. Gray filled circles denote R5-using strains and white filled circles X4-using strains.

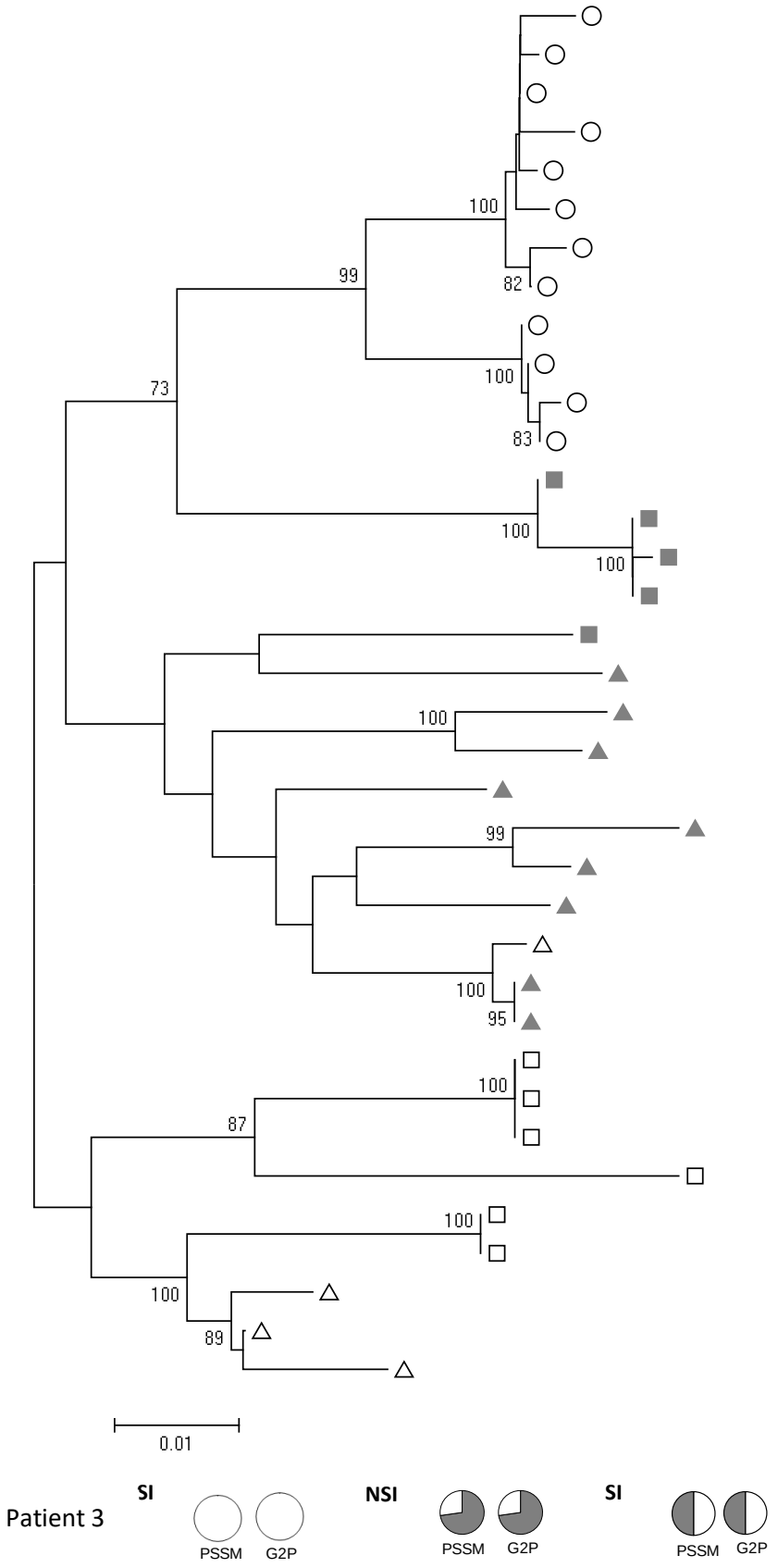

Figure 1C. Maximum likelihood phylogenetic trees of proviral nucleotide sequences of C2-V5 *env* gene showing sampling time and tropism. The quasispecies present: at 12-years old are shown by circles, at 16-years old are

shown by triangles and at 19-years old are shown by squares. Filled symbols correspond to R5-using strains while empty symbols to X4-using variants. The figure under the phylogenetic tree represents the proportion of X4 and R5 HIV-1 strains patient 3 at different times of infection studied by molecular cloning. Gray filled circles denote R5-using strains and white filled circles X4-using strains.

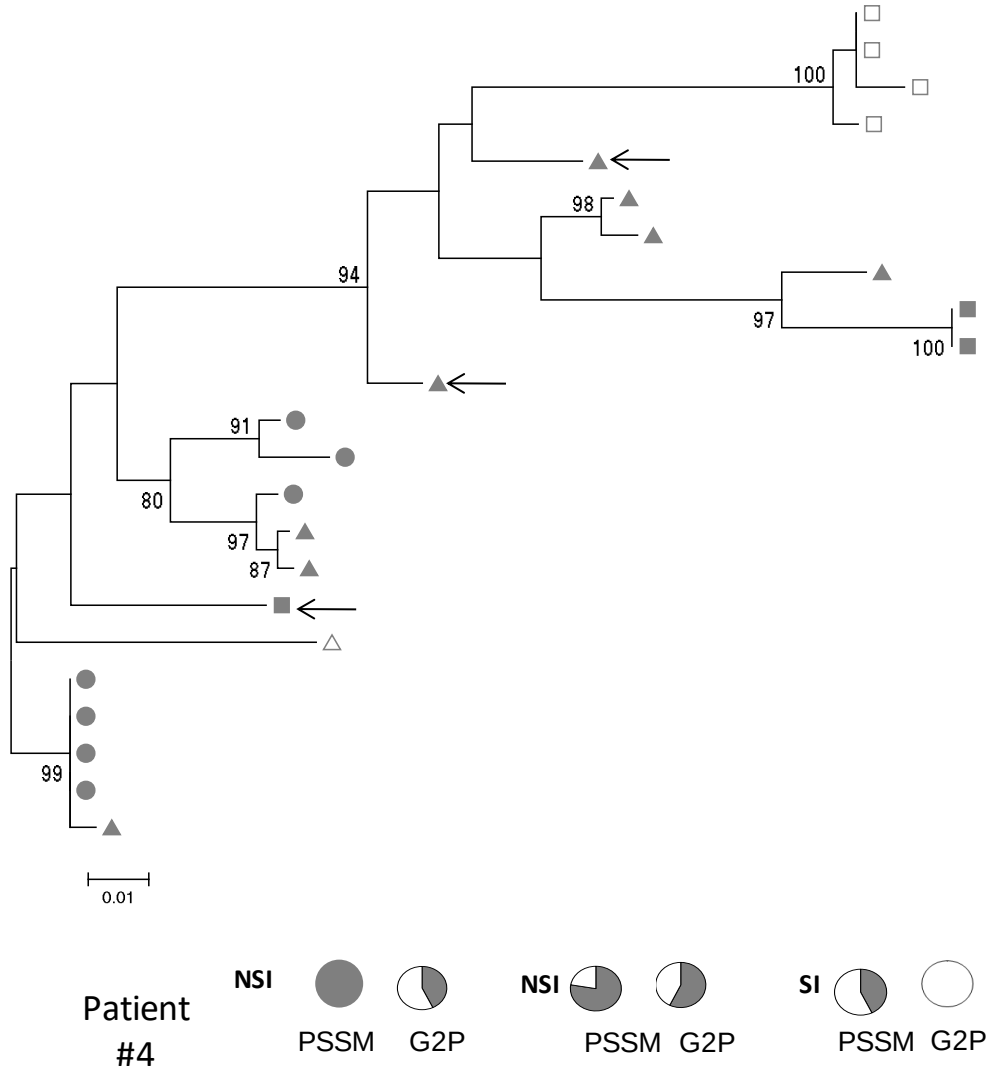

Fig 1D. Maximum likelihood phylogenetic trees of proviral nucleotide sequences of C2-V5 HIV *env* gene showing sampling time and tropism. The arrows indicate the sequences that have discordances between the PSSM and Geno2pheno. The quasispecies present: at 9-years old are shown by circles, at 13-years old are shown by triangles and at 15-years old are shown by squares. Filled symbols correspond to R5-using strains while empty symbols to X4-using variants. The figure under the phylogenetic tree represents the proportion of X4 and R5 HIV-1 strains patient 4 at different times of infection studied by molecular cloning. Gray filled circles denote R5-using strains and white filled circles X4-using strains.

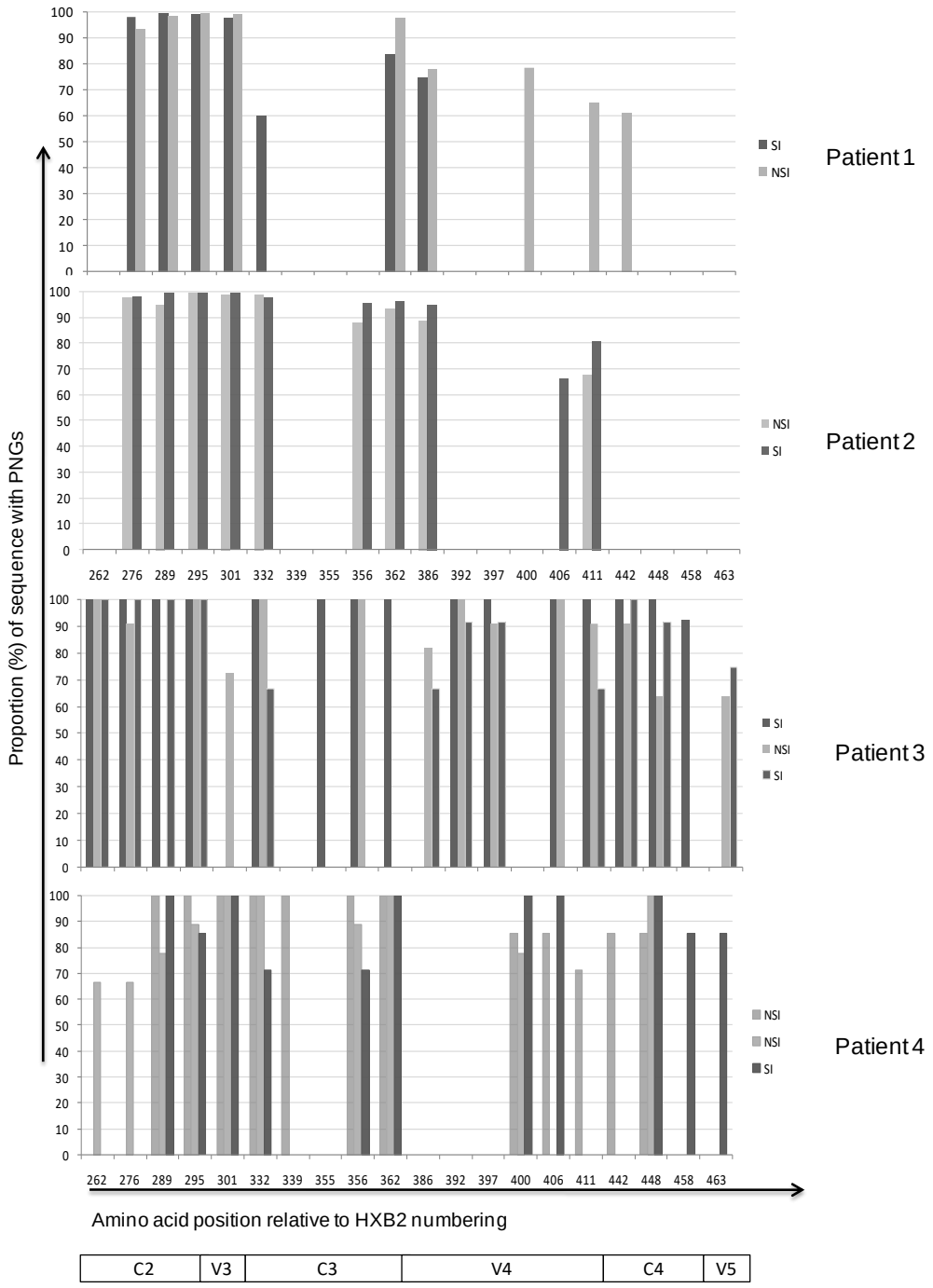

Fig 2. Frequency of PNGs in C2-V5 region of HIV *env* for each patient time point. The bars in grey color represent NSI time points and black bars shown the SI time points. Amino acid positions are numbered according to HXB2 reference strain.

Table 1. Characteristics of the viral phenotype at each of the study time points in 4 HIV-1 vertically infected children/ adolescents

Patient ID	Time of the study/ Age (y.o)	HIV RNA load (log 10 copies)	%CD4	CDC stage	Viral phenotype	PSSM-prediction by molecular cloning	
						X4-using strains (%)	R5-using strains (%)
1*	t_1= 3	5,90	39	C	SI	0	100
	t_2= 4	4,12	37	C	NSI	0	100
2*	t_1= 10	5,43	10	C	NSI	100	0
	t_2= 11	5,50	6	C	SI	100	0
3	t_1=12	4,68	15	C	SI	100	0
	t_2= 16	5,83	18	C	NSI	25	75
	t_3= 19	5,16	21	C	SI	50	50
4	t_1= 9	3,90	32	B	NSI	0	100
	t_2= 13	3,80	39	B	NSI	25	75
	t_3= 15	5,43	28	B	SI	55	45

*Patient analyzed by molecular cloning and NGS

Table 2: Genotypic determinants associated to of SI/ NSI phenotype in HIV-1 longitudinal samples from 4 individuals

	Patient 1		Patient 2		Patient 3			Patient 4			
	SI	NSI	NSI	SI	SI	NSI	SI	NSI	NSI	SI	
Position	AA (%)	AA(%)	AA (%)	AA(%)	AA (%)	AA(%)	AA (%)	AA (%)	AA(%)	AA (%)	Region
336	E (1%)	E(74.9%)						G (100)	G(44.4%)	G (14.3%)	**C3**
	G (22.1%)	G (1.5%)						R (0)	R(44.4%)	R (0)	
	R (77.8%)	R (23.6%)						K (0)	K (11.1)	K (85.7)	
340					E (0)	E (36.4)	E (0)	N (42.9)	N (22.2)	N (0)	**C3**
					K (100)	K (63.6)	K (83.3)	K (42.9)	K (66.7)	K (14.3)	
					N (0)	N (0)	N (16.7)	E (11.1)	E (11.1)	E (85.7)	
341	K (55.8)	K (86.7)			K (100)	K (45.5)	K (83.3)				**C3**
	E (0.4)	E (0.2)			N (0)	N (27.3)	N (0)				
	T (28.4)	T (3.3)			Q (0)	Q (27.3)	Q (16.7)				
	M (0.5)	M (0.4)									
	GAPS (15)	GAPS (9.7)									
343	K (45.0)	K (76.6)						H (42.9)	H (22.2)	H (0)	**C3**
	E (31.4)	E (22.3)						Q (57.1)	Q (11.1)	Q (14.3)	
	A (23.5)	A (0.8)						K (0)	K (66.7)	K (28.8)	
	Q (1)	Q (0.3)						R (0)	R (0)	R (57.1)	
346	R (41.9)	R (76.1)			K (100)	K (63.6)	K (91.7)	K (100)	K (44.4)	K (14.3)	**C3**
	K (55.8)	K (5.3)			Q (0)	Q (0)	Q (8.3)	A (0)	A (33.3)	A (85.7)	
	G (2.2)	G (18.6)			R (0)	R (9.1)	R (0)	G (0)	G (11.1)	G (0)	
					T (0)	T (18.2)	T (0)	E (0)	E (11.1)	E (0)	
402	D (50.7)	D (74.5)						N (100)	N (66.7)	N (14.3)	**V4**
	N (7.0)	N (13.9)						S (0)	S (33.3)	S (85.7)	
	G (8.9)	G (1.3)									
	K (20.8)	K (3.1)									
	- (12.6)	- (7.3)									
412	N (42.5)	N (75.4)	N (59.6)	N (84.4)							**V4**
	D (22.3)	D (3.2)	T (3.8)	T (3.8)							
	- (35.2)	- (21.5)	K (1.1)	K (0)							
			D (9.5)	D (0.8)							
			- (23.5)	- (11.0)							
459					N (100)	N (45.5)	N (100)	S (66.7)	S (0)	S (0)	**C4**
					R (0)	R (9.1)	R (0)	N (33.3)	N (28.6)	N (14.3)	
					T (0)	T (18.2)	T (0)	T (0)	T (57.1)	T (85.7)	
					- (0)	- (27.3)	- (0)				
460			N (32.0)	N (19.5)	E (30.8)	E (18.2)	E (50)				**V5**
			K (0.8)	K (34.5)	G (0)	G (41.7)	G (8.3)				
			- (67.3)	- (46.0)	K (61.5)	K (0)	K (41.7)				
					N (0)	N (9.1)	N (0)				
					R (7.7)	R (0)	R (0)				
					- (0)	- (25)	- (0)				

Highlights

- Vertically infected patients show HIV-1 phenotypic switch by the MT-2 assay.
- In half of the subjects, co-existence of X4 and R5-using strains was identified.
- Nine novel determinants of HIV-1 tropism in subtype F C2-V5 env were found.
- No association between HIV-1 quasiespecies evolution and tropism over time.

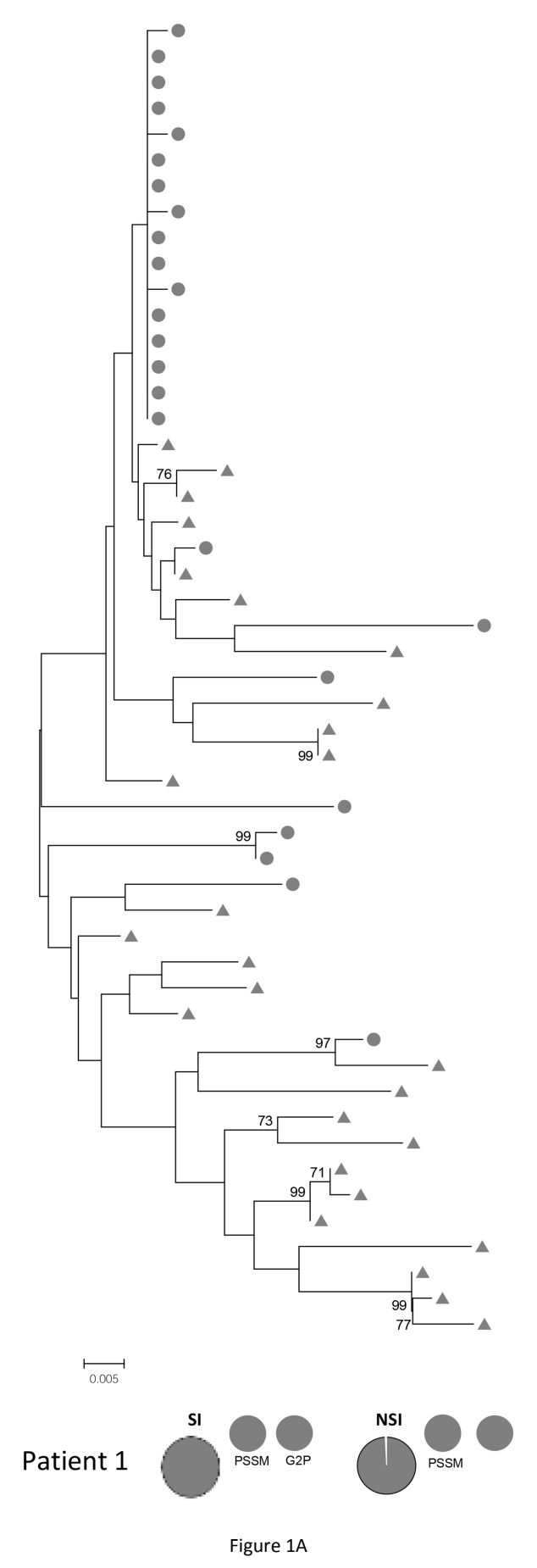

Figure 1A

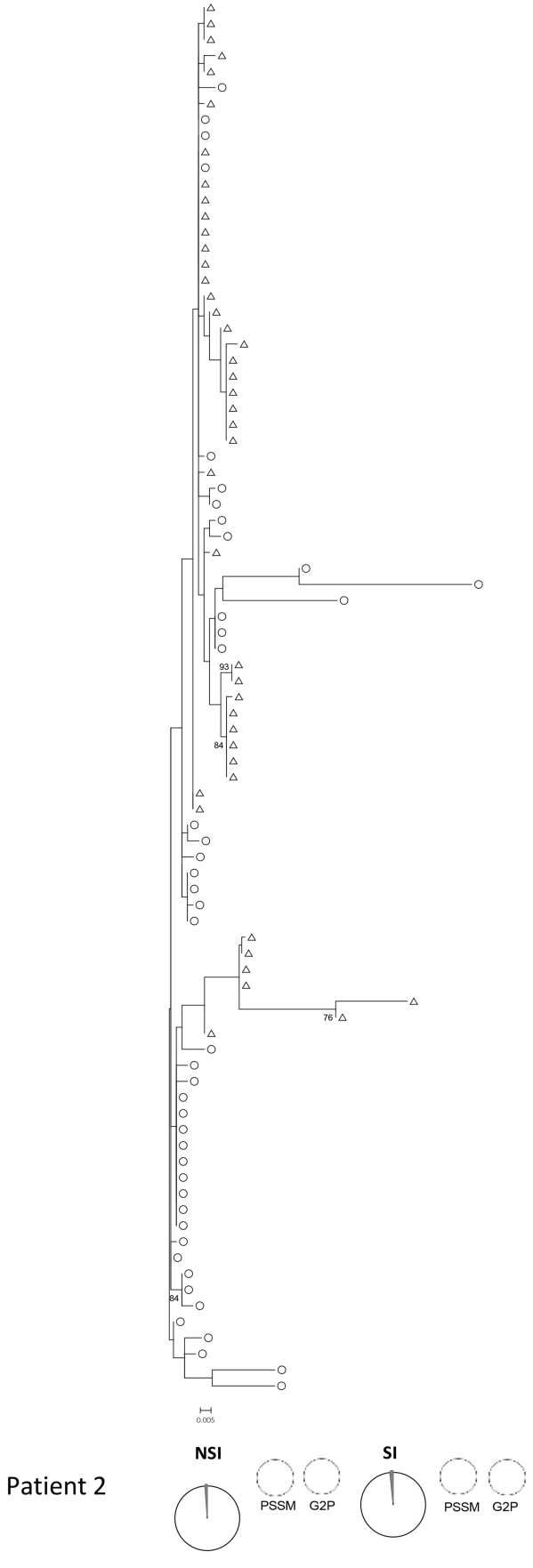

Patient 2

Figure 1B

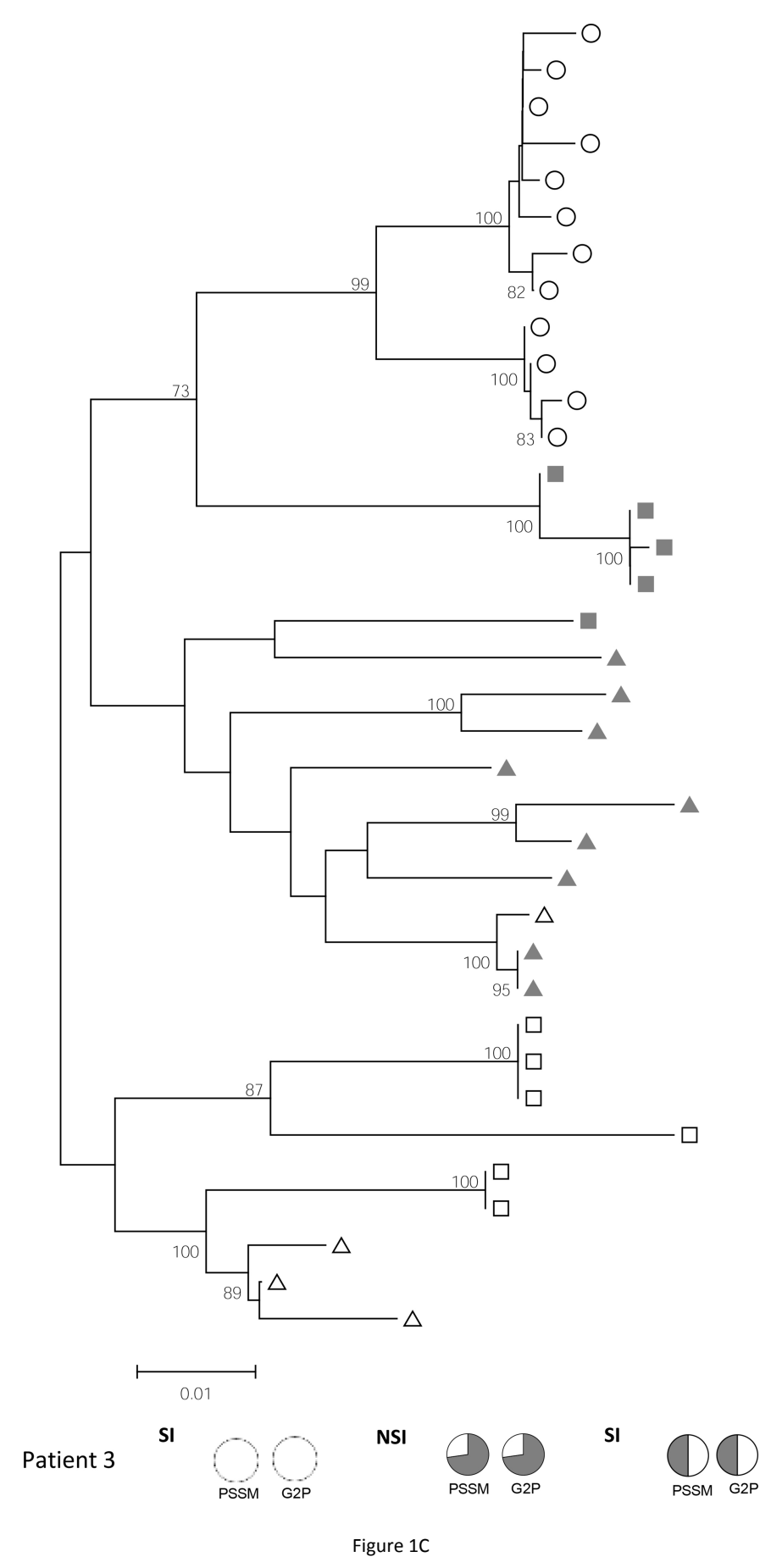
100
99
82
100
73
83
100
100
100
99
100
95
100
87
100
100
89
0.01
Patient 3
SI
PSSM
G2P
NSI
PSSM
G2P
SI
PSSM
G2P

Figure 1C

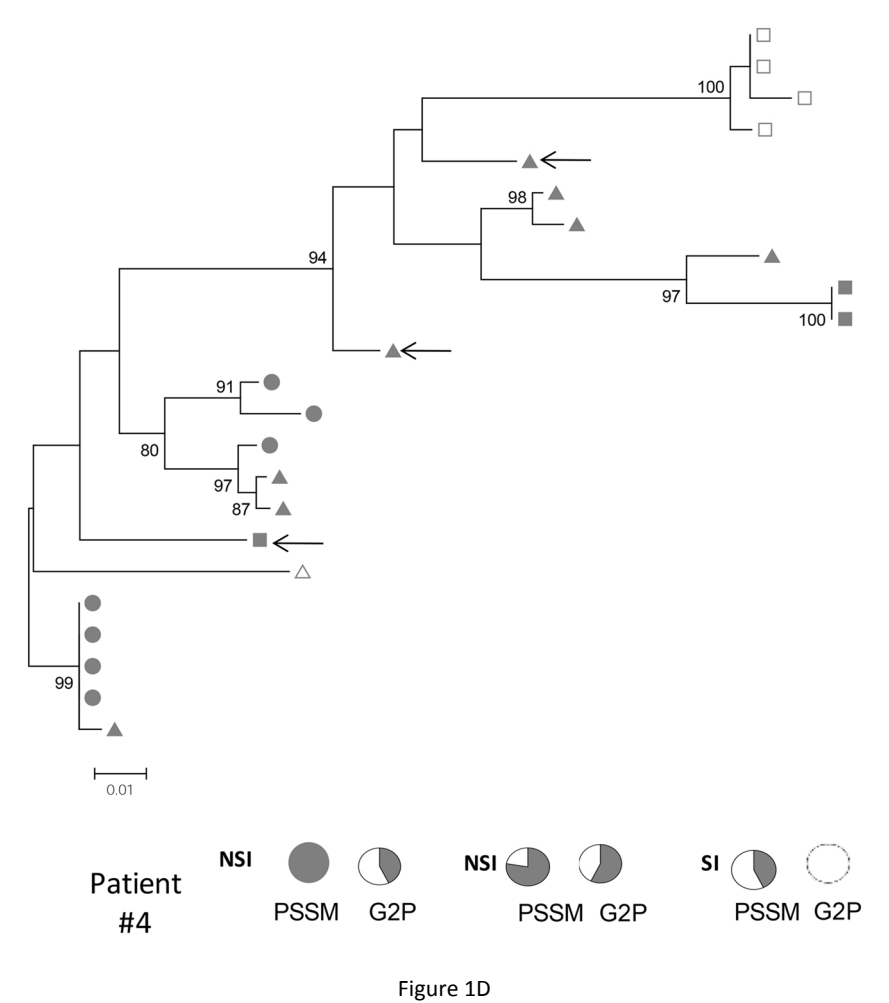
100
98
94
97
100
91
80
97
87
99
0.01
Patient #4
NSI
PSSM
G2P
NSI
PSSM
G2P
SI
PSSM
G2P

Figure 1D

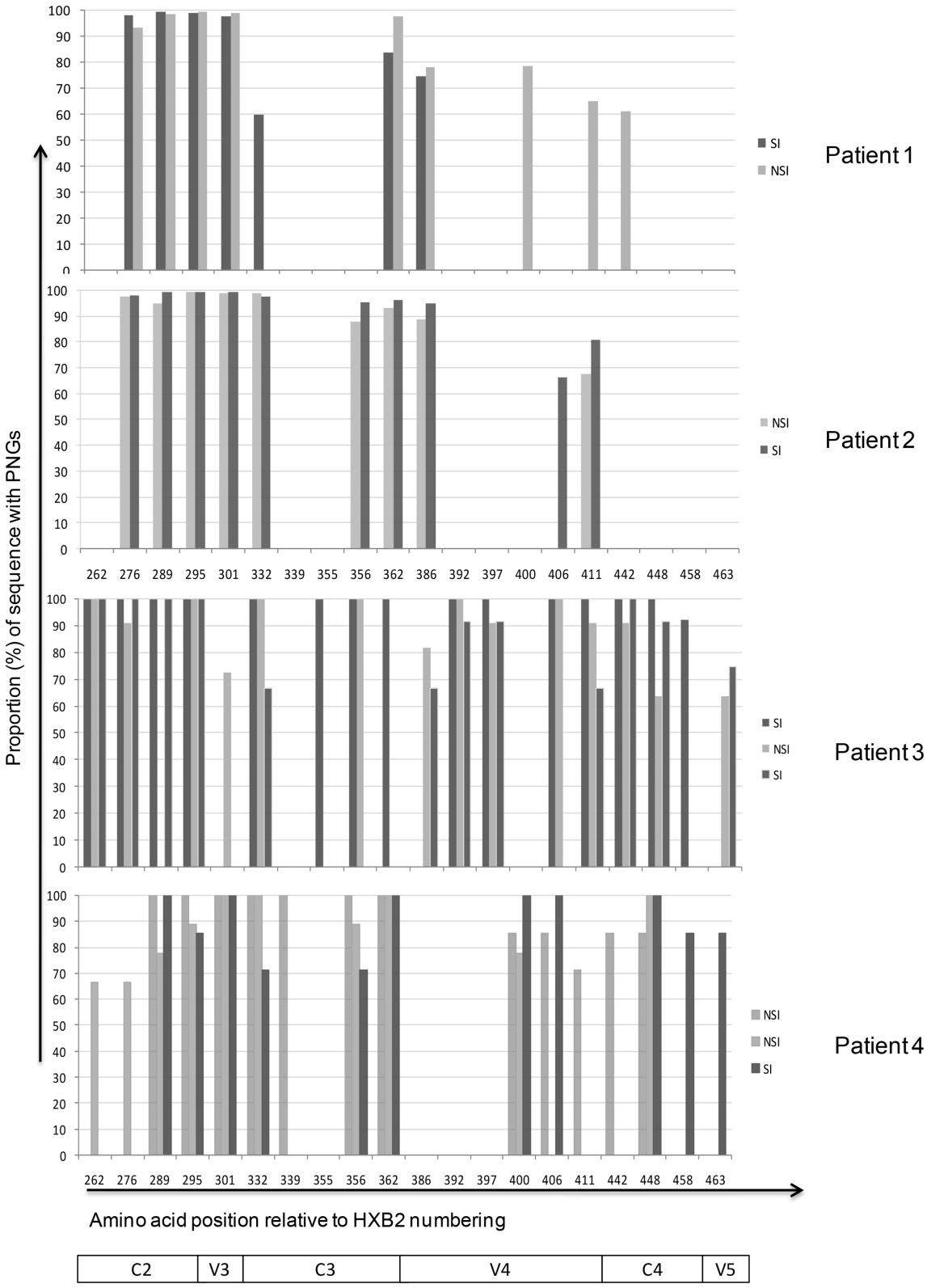
Proportion (%) of sequence with PNGs
Patient 1
SI
NSI
Patient 2
NSI
SI
Patient 3
SI
NSI
SI
Patient 4
NSI
NSI
SI
262 276 289 295 301 332 339 355 356 362 386 392 397 400 406 411 442 448 458 463
Amino acid position relative to HXB2 numbering
C2
V3
C3
V4
C4
V5

Figure 2